LOGIC
Journal of Engineering Design and Technology
Vol. 26 No. 1 March 2026 ; p. 48 - 60

p-ISSN : 1412-114X
e-ISSN : 2580-5649
http://ojs2.pnb.ac.id/index.php/LOGIC

PROTOTYPE DESIGN OF BATTERY CHARGING SYSTEM WITH THE USE OF REPEATED WATER CYCLE AT PICOHIDRO POWER PLANT

Marianus Nofu [1)], Frans J. Likadja [1)*], Almido H. Ginting [1)]

1) Department of Electrical Engineering, Faculty of Science and Engineering, Nusa Cendana University, Kupang, Indonesia

Corresponding email [1)*] : Frans.likadja@staf.undana.ac.id

Abstract. Pico Hydro Power Plants are small-scale hydropower systems with capacities below 5 kWs that have significant potential as renewable energy sources, particularly in remote areas. However, their implementation is often constrained by fluctuations in water discharge during the dry season, which lead to a decline in system performance. This study aims to design and experimentally evaluate a prototype battery charging system utilizing a repeated water cycle in a Pico Hydro Power Plants to enhance energy supply sustainability. The experimental method was employed by developing a system consisting of a water pump, Pelton turbine, DC generator, smart valve, solar charge controller (SCC), time relay, solar panels, and batteries as energy storage. Experimental testing was conducted by analyzing generator output under various water head and discharge conditions and comparing it with the pumped water discharge within a closed-loop cycle. The results indicate that at a head of 3.9 m, the generator produced an output of 1.7 V and 2.4 A, resulting in a battery charging time of 22.7 hours, whereas at a higher head of 5.42 m, the charging time was reduced to 11.01 hours. In addition, the solar panel system was able to supply the initial load during the system startup process before the pico hydro system is fully operated. Although the proposed system still exhibits limitations in charging time efficiency, the prototype demonstrates good conceptual and functional system integration, indicating strong potential for further development through design optimization to improve overall system efficiency and performance.

Keywords : Picohydro Power Plant*, Water Pump, Smart Valve, Solar Panels, Pelton Turbine, DC Generator, Relay Time, Battery*

1. INTRODUCTION

The increasing demand for sustainable energy and the growing awareness of environmental degradation have accelerated the global transition from fossil-based energy sources to renewable energy technologies [1], [2]. Conventional fossil fuels are associated with significant environmental impacts, including air pollution, greenhouse gas emissions, and long-term ecological degradation [3]. Consequently, renewable energy systems are increasingly promoted as environmentally friendly alternatives capable of supporting sustainable development.

Despite their advantages, renewable energy sources usually had challenges related to intermittency and resource availability [4]. Solar photovoltaic systems experience power fluctuations due to weather conditions and diurnal cycles [5], geothermal power plants are constrained by high capital costs, regulatory limitations, and location-specific requirements [6], while conventional hydropower systems are often suffer from reduced water discharge during dry seasons. These limitations are inhibitting the continuity and reliability of renewable energy supply, particularly in remote or off-grid areas.

Pico-hydropower plants represent a promising solution for decentralized electricity generation due to their simple construction, low environmental impact, and suitability for small-scale applications [7], [8]. However, the performance of pico-hydropower systems is highly dependent on continuous water availability. During periods of low discharge, such as the dry season, power generation capability decreases significantly, limiting their effectiveness as a reliable energy source [9]. Previous studies on pico-hydropower systems have predominantly

focused on turbine design optimization [10], [11], electrical performance enhancement [12], [13], or hybridization with other renewable sources while relatively,only a little attention has been given to addressing water availability constraints through integrated system-level approaches.

To address this research gap, this study proposes a prototype pico-hydropower system employing a repeated water cycle combined with battery energy storage and time-based control. The proposed system utilizes two reservoirs with different elevations, an automatic valve, and a water pump to circulate water continuously in a closed-loop configuration. A time-based control strategy is implemented to regulate the alternating operation of the pump and turbine, ensuring that energy consumption and energy generation do not occur simultaneously. This approach aims to enhance operational continuity and improve energy sustainability, particularly during periods of limited natural water discharge.

Therefore, the objective of this study is to design and experimentally evaluate the performance of a battery charging system for a pico-hydropower plant using a repeated water cycle. The evaluation focuses on system feasibility, operational continuity, and electrical performance under varyated head and water discharge conditions.

2. METHODS

This study was conducted by designing and experimentally testing a pico-hydropower plant prototype based on a repeated water cycle system. The system was designed to utilize water energy in a circulatory manner, in which the generator output was used to supply electrical loads during nighttime operation while simultaneously recharging the battery as an energy storage. Experimental testing was carried out to evaluate system performance under specific head and water discharge conditions.

The system consisted of a solar panel, solar charge controller (SCC), battery, water pump, Pelton turbine, DC generator, automatic valve (smart valve), CN101A digital time relay, double time delay relay (TDR) modules, a buck–boost DC converter, and a diode for unidirectional current protection. The DC generator used in this study had a nominal power rating of 250 watt with an operating voltage of 12 Volt DC, selected according to the characteristics of small-scale pico-hydropower systems and the experimental conditions. The Pelton turbine converted the kinetic energy of the water flow into mechanical energy, which was subsequently converted into direct current (DC) electrical energy by the DC generator. Water flow regulation toward the turbine was controlled using a 12 V DC solenoid valve (smart valve). Energy storage was provided by a 12 V battery with a capacity of 6,5 Ah, while the generator output voltage was regulated using a buck–boost converter before being supplied to the SCC and the load.

The system operated automatically based on time-based control, with the CN101A digital time relay serving as the main control unit. During the initial stage, the solar panel charged the battery through the SCC until a fully charged condition was reached. When the time reached 18:00, the CN101A relay activated the pico-hydropower system and shifted the energy source from the solar panel to the battery to support nighttime operation.

To prevent a simultaneous operation between the pump and the turbine and to improve system efficiency, a time-based control strategy employing two independent time delay relay (TDR) modules was implemented. The first TDR controlled the operation of the water pump, while the second TDR controlled the opening and closing of the automatic valve. During the filling phase, the water pump was activated for 1 minute and 54 seconds to transfer water from the lower reservoir to the upper reservoir, while the automatic valve remained closed to prevent water flow toward the turbine. Conversely, during the discharge phase, the automatic valve was opened for 22 seconds to allow water to flow from the upper reservoir to the Pelton turbine, while the water pump was deactivated. This operating scheme ensured that energy consumption by the pump did not occur simultaneously with the energy generation process of the turbine.

The mechanical energy produced by the Pelton turbine is being converted into DC electrical energy by the generator and utilized to supply the load while simultaneously recharging the battery. A diode was installed to ensure unidirectional current flow and to prevent reverse current from flowing back to the generator. After passing through the turbine, the water was collected in a secondary reservoir and subsequently pumped back to the primary reservoir using a 12 V DC water pump, enabling continuous operation in a closed-loop water cycle until 05:00. At this time, the CN101A relay deactivated the pico-hydropower system, and the system returned to battery charging mode using the solar panel.

The control system applied in this study was classified as an open-loop control system, as it did not utilize feedback sensors such as water level or flow rate sensors. The time-based control approach was selected to simplify the prototype design and to focus the study on evaluating the feasibility and performance of the pico-hydropower system that uses a repeated water cycle concept. Overall system of this pico-hydro power plant can be seen in

Figure 1 below.

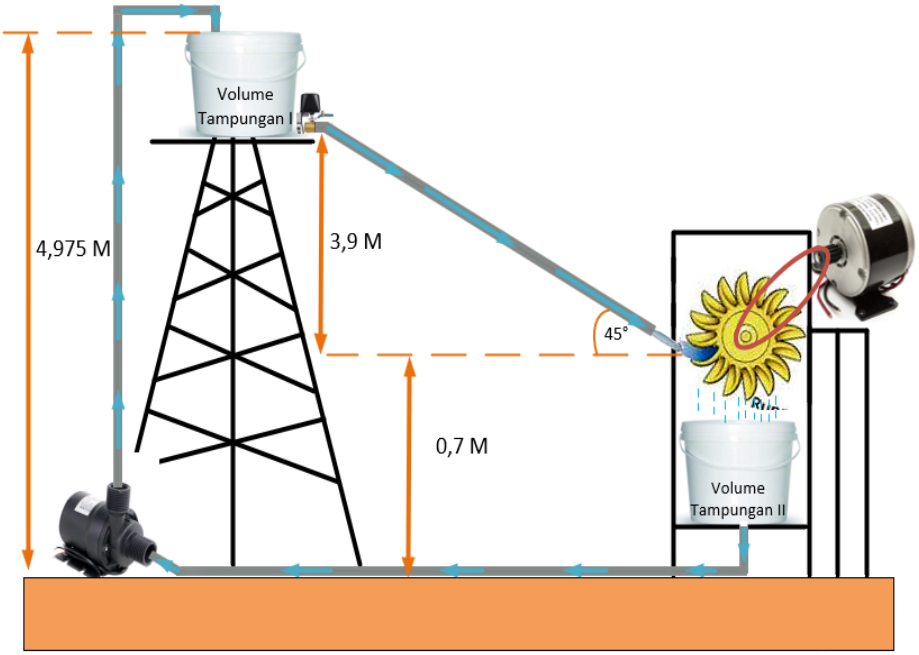

Figure 1. Building model of a picohydro power plant with repeated water cycle

3. RESULTS AND DISCUSSION

3.1 Solar Panel Input and Output Analysis

The output power testing of the 30 WP x 2 solar panel was done on May 8, 2025 with the following results:

Table 1. Solar Panels Output

Time	Voltage (V)	Current (A)	Power (Watt)	Sunlight Intensity (LUX)	Temperature (°C)
08:30AM	21,07	0,795	16,75065	65280	27°C
09:00AM	20,88	1,037	21,65256	99690	29°C
09:30AM	20,42	0,297	6,06474	15920	31°C
10:00AM	20,58	2,159	44,43222	175700	31°C
10:30AM	20,69	1,571	32,50399	173100	31°C
11:00AM	20,19	2,671	53,9749	177000	30°C
11:30AM	20,27	2,568	52,05336	182500	30°C
12:00AM	19,67	1,829	35,97643	125600	30°C
12:30AM	19,48	0,43	8,3764	21370	32°C
13:00AM	20,53	1,739	35,70167	170800	32°C
13:30AM	20,83	1,94	40,4102	173800	33°C
14:00AM	19,47	2,093	40,75071	145900	33°C
14:30AM	19,45	1,108	21,5506	92040	32°C
15:00AM	19,61	0,916	17,96276	85230	33°C
15:30AM	19,87	0,758	15,06146	128400	32°C
16:00AM	19,72	0,429	8,45988	81000	32°C
16:30AM	17,12	0,038	0,65056	2823	32°C
Average	19,99	1,316	27,605	112714,88	31,17°C

The measurements were conducted using a photovoltaic panel installed at a fixed tilt angle of 10° and oriented toward the north. The measurement results presented in Table 1 indicate significant power fluctuations within relatively short time intervals. For instance, at 09:00, the output power was recorded at 21.65 W, then dropped sharply to 6.06 W at 09:30, before increasing rapidly to 44.43 W at 10:00. A similar fluctuation pattern was also observed at 12:30, followed by a significant increase at 13:00. This behavior reflects the intermittent nature of photovoltaic power generation under real field operating conditions.

These power fluctuations were not caused by load variations, but were primarily attributed to the variability of solar radiation received by the photovoltaic module. During the morning to late morning period, rapidly moving cloud cover (passing clouds) caused sudden decreases and increases in the solar radiation incident on the panel. This phenomenon is reflected in the measured light intensity data, which also exhibit significant variations over the same period intervals.

It should be noted that the output current of the photovoltaic panel is highly sensitive to changes in solar radiation, whereas the output voltage remains relatively stable. This trend is evident in the measurement data, where extreme power fluctuations are mostly caused variations in current rather than voltage. This observation matched with the theoretical characteristics of photovoltaic modules, in which the output power is directly related to the photocurrent generated by solar radiation.

The observed power fluctuations shows one of the primary challenges of photovoltaic systems, which is their intermittent and unstable nature, which emphasized the need for mitigation strategies to enhance system reliability in practical applications. The data related to the solar panel output can be seen in the graph below:

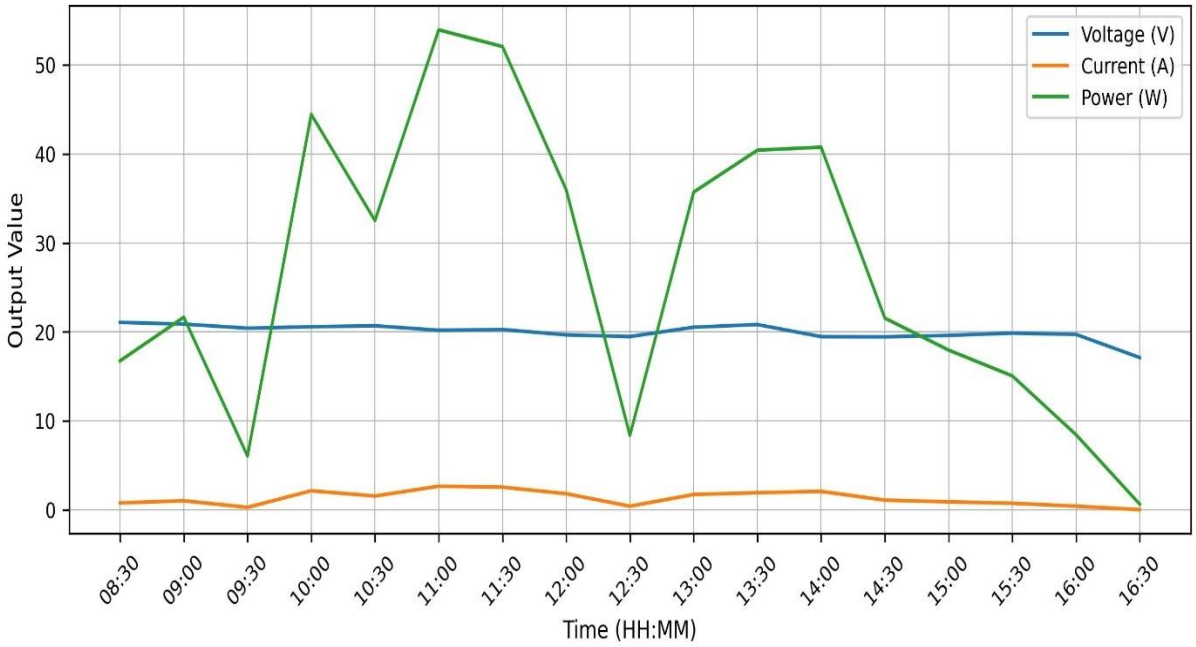

Figure 2. Solar Panels Output Graph

3.2. Energy Testing of Falling Water

3.2.1. Water discharge

Water discharge is the volume of water that passes through a cross-sectional area in one unit of time [14]. In this test, the volume of the water reservoir at the top is equal to the volume of water below. The reservoir used is in the shape of a tube with a radius of 15 cm and a height of 7.5 cm. Based on the existing data, the volume of the reservoir is calculated as follows:

$$V\ Tube = \pi . r^2 t \quad (1)$$

Then Tube volume = 3.14 x 152 x 37.5= 0.02649 m^3.

The period required to empty the reservoir in a full state with a height of 3.9 meters is 22 seconds. After calculating the volume and period required for emptying the reservoir, the flow rate can be calculated using the following equation

$$Q = \frac{v}{t}; \text{ or } Q = Av \quad (2)$$

water flow rate(Q) = 0.02649/22= 0.0012 m^3/s.

3.2.2. Water Flow Speed

The speed of the water flow out of the water reservoir depends on the area of the sluice gate used. The sluice gate used in this test is circular in shape with a diameter of 20 mm. The equation for calculating the sectional area of the circle is as follows

$$A = \pi r^2 \quad (3)$$

Then the area of the sluice gate is:
A = 3.14 x 10 x 10= 0.000314 m^2.
After determining the area of the sluice, the flow speed can be calculated based on the following equation:

$$v = \frac{Q}{A} \quad (4)$$

the value of the water flow speed is:

0.0012/0.000314= 3.8216m/s

The flow speed on a nozzle with a diameter of 15mm can be calculated using the principle of continuity:

$$v_1 A_1 = v_2 A_2 \quad (5)$$

V2 = 0.001199/0.000176 = 6.812m/s

3.2.3. Water Power Analysis

The power generated by the flowing water can be calculated using the following equation:

$$P = \rho\, g\, Q\, H \quad (6)$$

P = 1000 x 9,8 x 0,0012 x 3,9 = 45,864 Watt

3.3. Turbine and Generator Analysis

3.3.1. Generator Analysis

This test is an experiment on a DC generator to see the output. In this test, a torque turbine transmission system was used using belts and pully. Before conducting the test, an analysis was carried out to see the amount of power that can be generated by the generator using equation 2.4 with the following analysis results:

$$P = \rho.g.Q.H.\eta g.\eta t \quad (7)$$

P = 1000 x 9,8 x 0,0012 x 3,9 x 0,85 x 0,78 = 0,0304 kWatt

The output of the generator this time is 1.7 Volts and also 2.4 A. The output power itself can be calculated as follows

P = V.I = 1,7 x 2,4 = 4,08 Watt.

$$\eta = \frac{P\ out}{P\ in} \times 100\% \quad (8)$$

$$\eta = \frac{4{,}08}{45{,}86} \times 100\% = 8{,}9\%$$

Based on the calculation results, the overall system efficiency is relatively low, reaching only 8.9%. This value indicates that several aspects of the system are contributing to the poor energy conversion performance. These aspects include the generator characteristics, the mechanical energy transmission system between the turbine and the generator, and the turbine performance itself.

The low generator output voltage of 1.7 V indicates that the generator is not operating at its optimal rotational speed. In a pico hydro power generation system, the generator performance is strongly influenced by rotational speed (RPM). In principle, the magnitude of the electromotive force (EMF) generated is proportional to the rotor speed. If the RPM is low, the generated voltage will also be low. This condition suggests a possible mismatch between the generator specifications and the relatively low head condition of 3.9 meters. The generator used likely requires a higher rotational speed to reach its nominal voltage.

Furthermore, the mechanical transmission system using a belt and pulley plays an important role in determining the final rotational speed delivered to the generator. If the pulley ratio is not designed to significantly increase the RPM, the turbine rotation will not be sufficient to meet the generator's speed requirements. An inadequate transmission ratio can cause the generator to operate far below its maximum efficiency point, resulting in low electrical power output.

Under a head condition of 3.9 meters, the system falls into the low-to-medium head category. Therefore, the selection of turbine type becomes a critical factor. Pelton turbines are generally more effective for higher head

applications, whereas for low-head conditions, crossflow or propeller turbines tend to be more suitable because they can utilize relatively low pressure and discharge more efficiently. If the selected turbine type is not well matched to the available head and discharge characteristics, the conversion of water potential energy into mechanical shaft energy will not occur optimally.

Thus, the low overall efficiency is not caused by a single factor, but rather by the cumulative energy losses occurring in the turbine, mechanical transmission system, and generator. Optimization of these three components has significant potential to improve the overall system performance

For comparison, tests were carried out using different discharges and heights to see the output voltage and current coming out of the generator. The test results are shown in the table 2:

Table 2. Table of Generator Output At Different Heights and Discharges

Height	Water Discharge	Voltage	Current
3,9 m	0,0008	0,626 V	0,776 A
3,9 m	0,0012	1,7 V	2,4 A
5,4 m	0,0012	2,5 V	2,973 A

3.3.2. Turbine Analysis

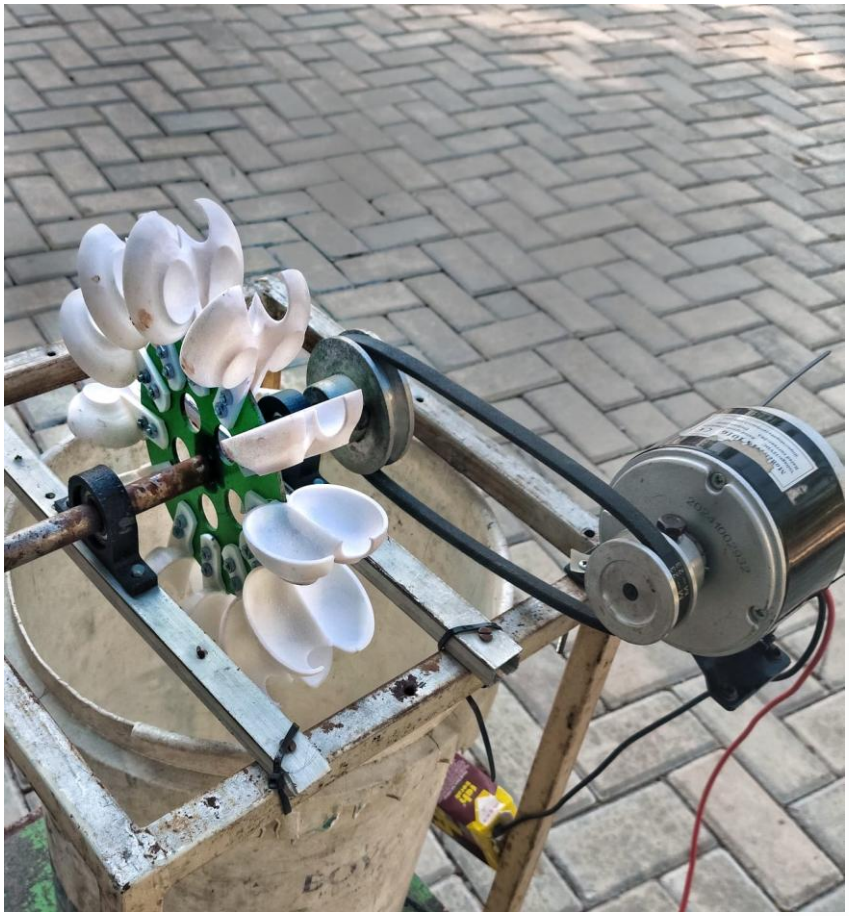

Figure 3. Turbine & Generator DC

In this study, a pelton turbine with 10 spoons was used like figure 3. The transmission system used is 3.5 inches on the turbine and 2 inches on the generator. Here's the Turbine Analysis:

A. Turbine Power

$$Pt = \rho . g . Q . H . \eta t \quad (9)$$

Pt = 1000 x 9,8 x 0,0012 x 3,9 x 0,85 = 0,03898kWatt

B. Speed Type of Turbine

$$n_s = n \cdot \frac{P^{\frac{1}{2}}}{H^{\frac{5}{4}}} \quad (10)$$

n = 458,3 rpm
P = V x I = 1,7 x 2,4 = 4,08 Watt = 0,00408 kW
$\sqrt{P} = \sqrt{0{,}00408} = 0{,}0639$
$N_s = \frac{458{,}3\ x\ 0{,}0639}{5{,}49} = 5{,}34$

Based on the calculation results, the specific speed (Ns) obtained is 5.3. This value is considered very low when compared to the general classification of water turbines. Theoretically, turbines with low specific speed values fall into the impulse turbine category, which are typically designed for high-head and low-discharge conditions. Therefore, the obtained Ns value indicates that the operating characteristics of the system tend to resemble those of a high-head impulse turbine.

However, the actual system condition only provides a head of 3.9 meters, which falls into the low-to-medium head category. This mismatch is an important indication that the turbine is not operating under optimal design conditions. Physically, the very low Ns value results from the combination of low output power (4.08 W) and relatively low rotational speed (458.3 rpm) compared to the available head. In fact, with a theoretical water power potential of approximately 45.9 W, the system should be capable of producing higher mechanical power and rotational speed if the energy conversion process were operating efficiently.

The low Ns value indicates that the water energy is not being fully converted into mechanical shaft power. This condition may be caused by several factors, such as a turbine design that is not well suited for low-head conditions, incomplete energy absorption by the turbine blades, or generator loading that restricts the increase in rotational speed. As a result, the mechanical power transmitted to the generator reduced, leading to low voltage and electrical power output.

Thus, the specific speed value of 5.3 does not merely classify the turbine characteristics, but also serves as an indicator that the system is operating far from its optimal operating point. The mismatch between turbine characteristics, available head conditions, and the loading system contributes significantly to the overall low system efficiency of 8.9%.

The test results with different discharges and altitudes for comparison in looking at turbine power and also the type speed of the test conducted are shown in table 3:

Table 3. Turbine Power Comparison Table And Type Speed At Different Discharge And Height

Height (m)	Water Discharge	Power (kW)	Speed Type Of Turbine
3,9	0,0008	0,000486 kW	1,54
3,9	0,0012	0,00408 kW	5,34
5,4	0,0012	0,00743	7,5

3.4. Cross-Section Pipe Analysis

The type of pipe used in this study is a 1/2 dim pvc pipe with a diameter of 18mm. 2 cross-sectional pipes are used, which are a cross-section of water falling towards the turbine and the pipe connected to the pump. Here are some analyses based on the cross-sectional pipe used

3.4.1. Reynold Number

If it is known that the diameter of the reservoir pipe used is 20mm = 0.02m and the kinematic viscosity value of water in a temperature of 30° = 0.804 x 10-6, as well as the water flow velocity that has been calculated beforehand, then by using the equation of 2.25, the value of the Reynolds number can bee calculated as follows [15]:

$$Re = \frac{VD}{\nu} \quad (11)$$

Re = 3,8216 x 0,02 / 0,804x10-6 = 9506,46

3.4.2. Mayor Losses

Major losses or losses of water friction with pipe walls need to be taken into account to see how much energy is lost [16]. To determine the magnitude of the loss due to friction or head major, we can used the following analysis:

$$H_{L(Mayor)} = f \frac{lv^2}{D.2.g} \quad (12)$$

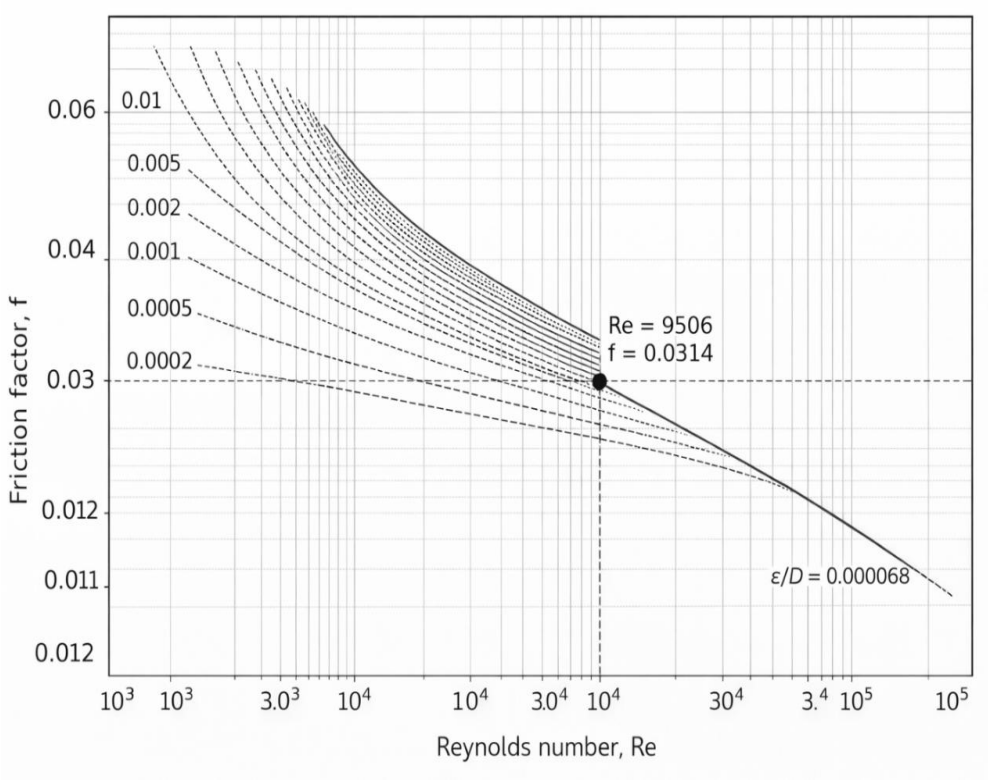

Figure 4. F value at the Moddy Chart cut-off point

Based on the image 4, the cut-off point representing the value of f is 0.0314. The value of Major losses is:

$$H_l = 0{,}0314\ x\ \frac{3{,}9\ x 3{,}8216^{\ 2}}{0{,}02\ x\ 2\ x\ 9{,}8} = 4{,}56\ m$$

3.4.2. Minor Losses

Minor losses are head losses caused by pipe turning, pipe shrinkage and the presence of nozzles. With turns, reductions and nozzles, it will affect the water power used [17]. To find out the magnitude of minor losses, we can used the following analysis:

$$H_{L(Minor)} = K\ \frac{v^2}{2g} \quad (13)$$

A. Minor Losses due to 45° turns

With the value of the minor losses coefficient 45° elbow= 0,4. The value of $H_{L(Minor)}$=

HL= 0,4 x (1,512/2 x 9,8) = 0,0465 m

B. Minor Losses Pipe to Tank

With the value of the minor losses coefficient Pipe to Tank= 1. The value of $H_{L(Minor)}$=

HL= 1 x (1,512/2 x 9,8) = 0,1163 m

C. Minor Losses Tank to Pipe

With the value of the minor losses coefficient Tank to Pipe= 0,5. The value of HL(Minor)=

HL= 0,5 x (1,512/2 x 9,8) = 0,0581m

3.5. Cycle of Ups and Downs of Water

To maintain the sustainability cycle of the water cycle continuously, it is necessary to pay attention to several things, including:

3.5.1. Pump Capacity and Pressure

In order to maintain the water sustainability cycle, the water discharge pumped from the bottom to the top is sufficient to compensate for the falling water discharge. Also, the pump pressure must also be considered

3.5.2. Loss of Pressure

The pressure loss is related to major and minor losses that will be analyzed later. Friction of the water flow with the pipe, the turn of the pipe or the overshok for a change in size can increase the possibility of pressure loss. One thing that should not be forgotten is the size of the pipe, which would be better balanced to match the water discharge fluctuations.

3.5.3. Control System

Integrated automatic control in regulating the pump, as well as the sluice gate is needed to maintain the stability of the water discharge in the cycle. Figure 5 illustrates the condition when the pico-hydropower system begins its operation. At this stage, the energy stored in the battery is used to supply the entire control circuit and system loads. The system operation is regulated by the CN101A digital time relay, which works as the main timer controller. When the time reaches 18:00, the CN101A relay automatically activates the pico-hydropower system and ensures that the energy source is switched to the battery to support nighttime operation.

To prevent simultaneous operation of the pump and the turbine and to improve overall system efficiency, a time-based control strategy was implemented using two independent Time Delay Relay (TDR) modules. The first TDR module controls the operation of the water pump, while the second TDR module regulates the opening and closing of the automatic valve (solenoid valve).

The system operates in two primary phases: the filling phase and the discharge phase. During the filling phase, the water pump is activated for 1 minute and 54 seconds to transfer water from the lower reservoir to the upper reservoir. During this period, the automatic valve remains closed to prevent water from flowing toward the turbine. Consequently, electrical energy is consumed solely for the pumping process, and no power generation occurs.

Conversely, during the discharge phase, the pump is deactivated and the automatic valve is opened for 22 seconds. Under this condition, water flows from the upper reservoir to the Pelton turbine, thereby generating electrical energy. This operating scheme ensures that energy consumption by the pump does not occur simultaneously with the turbine's power generation process. The time-sequenced operation prevents load conflict and enhances the overall efficiency and operational stability of the system. The Charging process with generator can be seen in the figure 6.

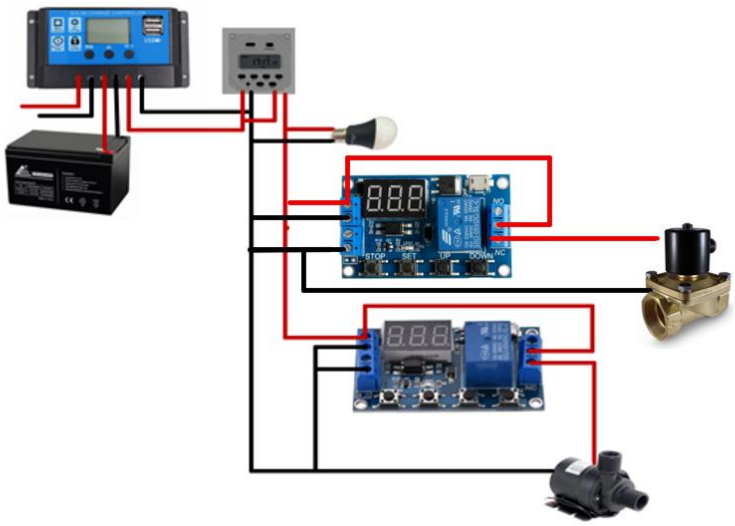

Figure 5. Control System In Load Manuvering

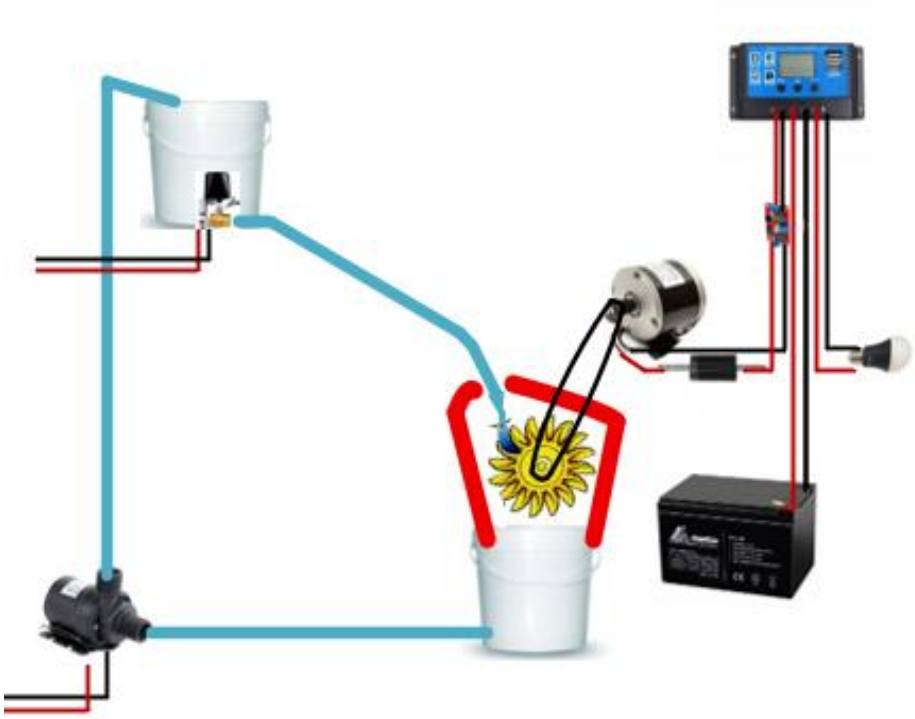

Figure 6. Charging with generator

3.6. Battery Charging Time Analysis

First, the battery discharge process is carried out to see the battery's ability to discharge the load. It is discharged for 6 hours using the load of the DC Pump without increasing the water with variable current between 0.313 A to 0.347 with the data in the table 4.

Table 4. Discharge Battery

Time	Current (A)	Voltage Battery (V)
08:15	0.313	12.58
09:00	0.33	12.48
09:45	0.347	12.36
10:30	0.32	12.22
11:15	0.34	12.1
12:00	0.325	11.98
12:45	0.313	11.9
13:30	0.33	11.84
14:15	0.347	11.8

After the battery discharge process is carried out to the battery voltage of 11.8V (SoC = ±30%), testing is carried out by carrying out the battery charge process.

3.6.1. Charging battery with solar panels

This process occurs during the day where the battery is charged first using a 2x30 WP solar panel. The charging process is shown in the table 5:

Table 5. Charging Baterry With Solar Panel

Voltage Baterry(V)	Current(A)	(W)	Charging Time
11.67	2.55	29.7585	13:00
11.8	2.49	29.382	13:11
11.92	2.6	30.992	13:23
12.03	2.5	30.075	13:34
12.15	2.58	31.347	13:45
12.28	2.45	30.086	13:56
12.38	2.6	32.188	14:08
12.42	2.42	30.0564	14:13
12.5	2.45	30.625	14:23
12.64			14:42

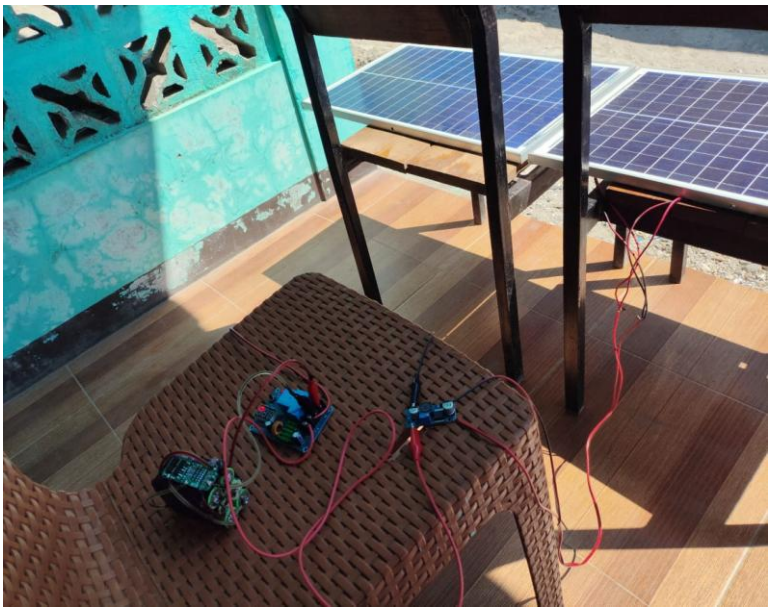

Figure 7. Charging Battery

3.6.2. Load maneuvering

When the time shows 18.00, the battery load turns on when the CN101A time relay starts to activate so that the load maneuver process from the solar panel to the water generator occurs. The maneuver begins with the pump raising water from the lower reservoir to the top by using the energy from a fully charged battery, which when the water rises to the upper reservoir the water will flow from the water reservoir through the smart valve to the cross-sectional pipe and then fall into the pelton turbine. For the pump and smart valve are controlled using a time delay relay (TDR).

3.6.3. Charging battery with Generator

2 tests were carried out at different heights to see the output of the generator to charge the battery with the following results:

A. Generator output at height of 3.9 m
- Generator Voltage: 1,6 V – 1,7 V
- Maximum Voltage of Generator: 1,767 V

- Generator current: 2,25 A – 2,42 A
- Peak Current: 2,427 A

Because the voltage is too low, a step up module is needed which is supported by the concept of power retention to get a charging voltage of 13.8 volts. In the use achieve the charging voltage is as follows:

$$P = V.I \quad (14)$$

P = 1,7 x 2,4 = 4,08 Watt

After getting power, we can analyze how much current can be used for charging, with the following analysis:

$$P = (V.I)\eta \quad (15)$$

I = (4,08/13,8) x 0,97 = 0,286 A

After the large charging current is obtained, the charging time, by [18] can be analyzed as follows:

$$h = \frac{Ah}{I} \quad (16)$$

h = 6,5/0,286 = 22,727 H

B. Generator output at height of 5.4 m

- Generator Voltage: 2,5 V - 2,6 V
- Maximum Voltage of Generator: 2,635 V
- Generator current: 2,9 A – 3,01 A
- Peak Current: 3,01 A

Because the voltage is too low, a step up module is needed which is supported by the concept of power retention to get a charging voltage of 13.8 volts. In the use achieve the charging voltage is as follows:

$$P = V.I$$

P = 1,635 x 3,1 = 7,931 Watt

After getting power, we can analyze how much current can be used for charging, with the following analysis:

$$P = (V.I)\eta$$

I = (7,931/13,8) x 0,97 = 0,59 A

After the large charging current is obtained, the charging time can be analyzed as follows:

$$h = \frac{Ah}{I}$$

h = 6,5/0,59

h = 11,01 H

4. CONCLUSION

This study successfully designed and implemented a time-based controlled pico-hydropower generation system integrated with a solar panel and battery as an energy storage unit. The system operation was controlled using a CN101A digital time relay as the main timing controller, along with two Time Delay Relay (TDR) modules to alternately regulate the operation of the water pump and the automatic valve.

The two-phase control strategy, consisting of a filling phase and a discharge phase, effectively prevented simultaneous operation of the pump and the turbine, ensuring that energy consumption and power generation did not occur at the same time. The system operated automatically according to the predefined time sequence, demonstrating the successful implementation of time-sequencing-based energy management.

However, experimental results indicate that the overall system efficiency remains relatively low at 8.9%. The specific speed (Ns) value of 5.3 suggests that the turbine's operating characteristics tend to resemble those of a high-head impulse turbine, while the actual system operates at a head of 3.9 meters, which falls within the low-to-medium head category. The mismatch between turbine characteristics, mechanical transmission system, and generator specifications is identified as the primary factor contributing to the low energy conversion performance.

Therefore, further optimization is required in terms of turbine selection, mechanical transmission ratio, and generator characteristics to better match the available head and discharge conditions. Future development is expected to improve system efficiency and enhance the feasibility of small-scale pico-hydropower systems with automated control strategies.

5. REFERENCES

[1] P. Lingkungan and Y. Berkelanjutan, "Green_Accounting_DAMPAK_TRANSFORMASI_ENERGI_HIJAU_," vol. 6, no. 1, pp. 1–9, 2025.

[2] B. A. S. Putri, G. V. A. Saroy, and R. K. Rajib, "Pendekatan peran hukum dalam mendorong transisi energi terbarukan," Jurnal Multidisiplin Ilmu Akademik, vol. 1, no. 3, pp. 230–235, 2024, doi: 10.61722/jmia.v1i3.1402.

[3] H. Tjiwidjaja and R. Salima, "Dampak energi fosil terhadap perubahan iklim dan solusi berbasis energi hijau," Jurnal Wilayah, Kota dan Lingkungan Berkelanjutan, vol. 2, no. 2, pp. 166–172, 2023, doi: 10.58169/jwikal.v2i2.625.

[4] F. M. Noor and A. F. Rahman, "Studi penerapan integrasi sumber energi baru terbarukan dengan smart grid dan sistem pengendalian SCADA," Proceedings of the Industrial Research Workshop and National Seminar, vol. 14, no. 1, pp. 526–532, 2023, doi: 10.35313/irwns.v14i1.5440.

[5] Siregar et al., "Pengaruh penggunaan teknologi superconducting magnetic energy storage (SMES) dalam sistem pembangkit energi listrik berbasis tenaga surya," Jurnal Media Informatika, vol. 6, no. 2, pp. 1545–1550, 2025, doi: 10.55338/jumin.v6i2.6533.

[6] E. Elfina and Z. Judge, "Kepastian hukum jaminan investasi energi terbarukan panas bumi dalam pengembangan energi di Indonesia," Jatijajar Law Review, vol. 2, no. 2, pp. 82–98, 2023, doi: 10.26753/jlr.v2i2.1156.

[7] B. Edi, S. Atifoqkymin, and M. Fitri, "Tinjauan literatur: kinerja turbin screw Archimedes pembangkit listrik tenaga pikohidro (PLTPH) pada aliran air dengan head rendah," Al-Jazari: Jurnal Ilmiah Teknik Mesin, vol. 9, no. 2, pp. 102–113, 2024, doi: 10.31602/al-jazari.v9i2.15853.

[8] D. Hamdani and M. L. Edypoerwa, "Study and design of picohydro power plant for low-head and low-flow application," ELKOMIKA: Jurnal Teknik Energi Elektrik, Teknik Telekomunikasi, dan Teknik Elektronika, vol. 13, no. 2, pp. 200, 2025, doi: 10.26760/elkomika.v13i2.200.

[9] M. I. Malik, W. Widyantoro, A. I. Rabbika, Y. Yanti, and Y. Yadi, "Analisis potensi pembangkitan listrik tenaga nano hydro di saluran irigasi Desa Cintaraja Tasikmalaya," Jurnal Teknik Elektro UNIBA (JTE UNIBA), vol. 9, no. 1, pp. 540–547, 2024, doi: 10.36277/jteuniba.v9i1.393.

[10] H. Haryadi, A. Mahmudi, Sugianto, and D. Setiawan, "Studi pengaruh debit dan jenis runner terhadap efisiensi turbin vorteks PLTPH," Jurnal PERMADI: Perancangan, Manufaktur, Material, dan Energi, vol. 5, no. 2, pp. 66–77, 2023, doi: 10.52005/permadi.v5i2.121.

[11] C. Flow, "5) , 1-5)," vol. 6, pp. 16–25, 2024.

[12] U. Amri, "Rancang bangun pembangkit listrik tenaga piko hidro (PLTPH) (analisis daya beban output pada generator)," Jurnal Tektro, vol. 5, no. 1, pp. 100, 2021, doi: 10.30811/tektro.v5i1.2803.

[13] U. Amri, Z. Zulfikar, and M. Mahalla, "Rancang bangun pembangkit listrik tenaga piko hidro (PLTPH) (analisis daya beban output pada generator)," Jurnal Tektro, vol. 5, no. 1, pp. 100, 2021, doi: 10.30811/tektro.v5i1.2803.

[14] N. P. V. Fitriyani, "Analisis Debit Air di Daerah Aliran Sungai (DAS)," *Ilmuteknik.org*, vol. 2, no. 2, pp. 1–10, 2022.

[15] M. Dzailani, "Analisis pengaruh sudut belokan terhadap head losses penstock di PLTA Timo 3×4 MW," 2023.

[16] F. Mujahid, "Pengaruh head losses mayor dan minor pada sistem instalasi turbin Pelton skala mikro," vol. 1, pp. 1–9, 2021.

[17] A. Minor, L. Alat, U. Aliran, and F. Skala, "Jurnal Dinamis Laboratorium," vol. 10, no. 2, pp. 7–19, 2022.

[18] Y. N. Hilal, P. Muliandhi, and E. N. Ardina, "Analisa balancing BMS (battery management system) pada pengisian baterai lithium-ion tipe INR 18650 dengan metode cut off," Simetris: Jurnal Teknik Mesin, Elektro dan Ilmu Komputer, vol. 14, no. 2, pp. 367–374, 2023, doi: 10.24176/simet.v14i2.9852.